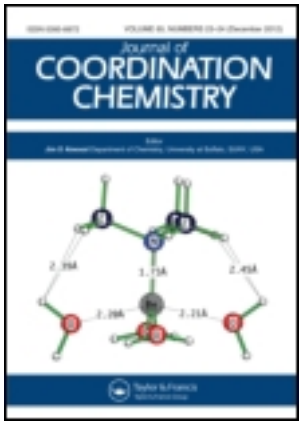

Journal of Coordination Chemistry
Publication details, including instructions for authors and subscription information:
http://www.tandfonline.com/loi/gcoo20

Meso-thienyl and furyl rotor effects in BF_2-chelated dipyrrin dyes: solution spectroscopic studies and X-ray structural packing analysis of isomer and congener effects

Taehong Jun [a], Kibong Kim [a], Kang Mun Lee [a], Andrew C. Benniston [b] & David G. Churchill [a]

[a] Department of Chemistry, Korea Advanced Institute of Science and Technology 373-1 Guseong-dong, Yuseong-gu, Daejeon 305-701, Republic of Korea

[b] Molecular Photonics Laboratory, School of Chemistry, Newcastle University, Newcastle-upon-Tyne, NE1 7RU, UK

Accepted author version posted online: 15 Oct 2012.Published online: 01 Nov 2012.

To cite this article: Taehong Jun, Kibong Kim, Kang Mun Lee, Andrew C. Benniston & David G. Churchill (2012) Meso-thienyl and furyl rotor effects in BF_2-chelated dipyrrin dyes: solution spectroscopic studies and X-ray structural packing analysis of isomer and congener effects, Journal of Coordination Chemistry, 65:24, 4299-4314, DOI: 10.1080/00958972.2012.740023

To link to this article: http://dx.doi.org/10.1080/00958972.2012.740023

Journal of Coordination Chemistry
Vol. 65, No. 24, 20 December 2012, 4299–4314

Meso-thienyl and furyl rotor effects in BF_2-chelated dipyrrin dyes: solution spectroscopic studies and X-ray structural packing analysis of isomer and congener effects

TAEHONG JUN†, KIBONG KIM†, KANG MUN LEE†, ANDREW C. BENNISTON‡ and DAVID G. CHURCHILL*†

†Department of Chemistry, Korea Advanced Institute of Science and Technology 373-1 Guseong-dong, Yuseong-gu, Daejeon 305-701, Republic of Korea
‡Molecular Photonics Laboratory, School of Chemistry, Newcastle University, Newcastle-upon-Tyne, NE1 7RU, UK

(*Received 10 August 2012; in final form 17 September 2012*)

Well-defined discrete fluorescent molecular systems with very subtle steric/electronic differences are interesting when considering solid-state packing and solution substituent effects. Herein, we report the synthesis and characterization of four 4,4-difluoro-1,3,5,7-tetramethyl-8-(C_4H_3X)-4-bora-3a,4a-diaza-*s*-indacene complexes ($X = O$, S). Various NMR spectroscopic experiments were used to assign all relevant atoms (CD_2Cl_2): ^{19}F, ^{11}B, ^{1}H, ^{13}C, ^{13}C–H undecoupled, ^{1}H–^{1}H COSY, ^{1}H–^{1}H NOESY, ^{1}H–^{13}C HSQC, and ^{1}H–^{13}C HMBC NMR spectroscopy. UV-Vis and fluorescence studies were undertaken for all compounds. Chemical shift differences were found between isomers and congeners; for congeners, aromatic δ differences were attributed to electron-poor character. Also, compounds **1**–**4** were studied crystallographically. In the solid state, internal dihedral planes and intermolecular packing patterns can be compared.

Keywords: Thienyl; Furyl; BF_2-dipyrrin; BODIPY; Isomers; Congeners; X-ray crystal structures; 2-D NMR spectroscopy

1. Introduction

The first derivative of the now-popular BF_2-chelated dipyrrin (BODIPY) fluorophore system was synthesized by Treibs and Kreuzer in 1968 [1]. Since that time, and in more recent years, a great variety of BODIPY (boradiazaindacene-type) species have been designed, synthesized, and characterized. Common substitutions at the pyrrolyl α-, β-, and dipyrrin *meso*-5-position are now well represented [2, 3]. Such BF_2-chelates now include a wide variety of simple substitutions, including alkyl/aryl groups, halides, as well as formal extensions of the aryl plane [2]. Some well-known fluorophores have been designed for labeling living cells [2–12]. Other practical efforts have led to fluorescent switches [13, 14], chemosensors [15–24], laser dyes [25], photosensitizers [26], energy transfer cassettes [27–29], and light harvesting arrays [30–33]. BODIPY dyes possess strong UV-Vis absorbing properties, sharp fluorescence emission profiles, and high

*Corresponding author. Email: dchurchill@kaist.ac.kr

ISSN 0095-8972 print/ISSN 1029-0389 online
http://dx.doi.org/10.1080/00958972.2012.740023

fluorescence quantum yields. Thus, much interest is centered on imminent and potential applications of this reliable system. BODIPY systems are relatively stable to physiological conditions and generally insensitive to their environments with respect to pH and solvent (polarity). Through all of these studies, the BODIPY class has gained increased exposure.

BODIPY systems have a common geometry (figure 1) and through strong BF_2-chelation can be considered as 5/6/5-membered fused ring systems, which leads to the *indacene* namesake. Common ring atom-numbering is shown for the BF_2-dipyrrin or boradiazaindacene core-based nomenclatures (figure 1). Part of the continued interest in derivatization involves the incorporation of heterocycles at the *meso*-position and their effect on fluorescence (colorimetric capacity). Aryl substituents in specific cases contain a "heavy" atom with the possibility to observe enhanced spin–orbit coupling. Hence, the overall intention is to systematize photophysical effects of single-point modifications (as a function of lighter/heavier congener) and formal isomerism in heterocycles. Steric effects and their bearing on photophysical effects have been reported [34]. Herein, a combined heteroatom and sterical effect study of 8-aryl-BODIPY systems stemming from 2,4-dimethylpyrrole was undertaken [35, 36]. The *meso*-position rotor when considering O-/S- congeners gives important information regarding certain electronic and steric parameters, and also crystallographic packing parameters relating to chalcogen/halogen placement of interest to materials chemistry and possibly to neurobiological probes. New and important photomolecular tools can emerge through simple heteroatom and rotor placement [35, 36]. BODIPY 8-furyl and 8-thienyl systems were first reported in 2007 [37, 38]. 8-Position multithienyl

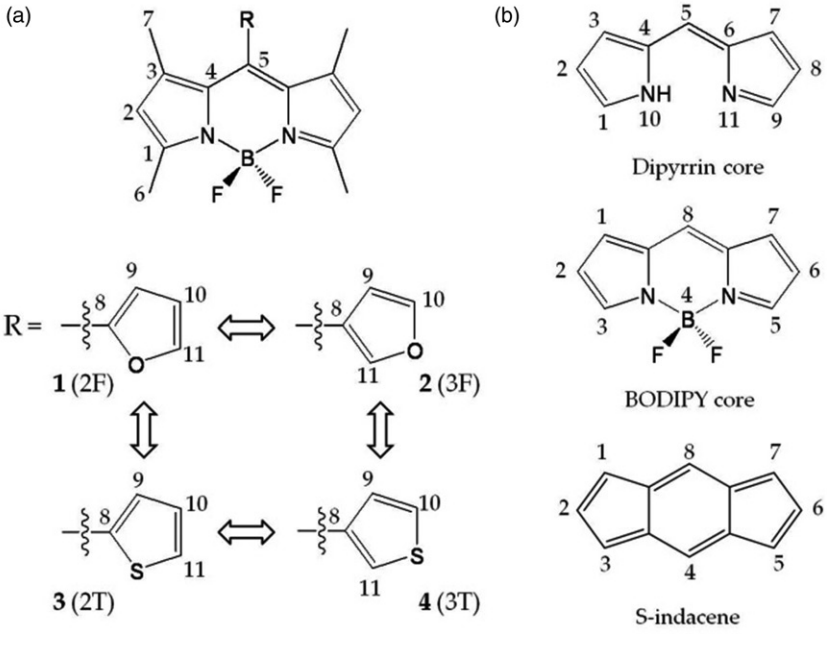

Figure 1. (a) Structures and atom-numbering for the four 4,4-difluoro-1,3,5,7-tetramethyl-8-(C_4H_3X)-4-bora-3a,4a-diaza-*s*-indacene ($X = O$, S) complexes synthesized and characterized herein. (b) Atom-labeling conventions: (top) numbering according to dipyrrin, (middle) BODIPY system, (bottom) *s*-indacene system.

conjugates [39–42], aniline-containing extensions [43, 44], and fluorophore extensions have also given the BF_2-chelates further versatility [45]. Reports of 3-thienyl [37, 46–49] and 3-furyl groups are fewer [46]. 2-Furyl reports often coincide with those for 2-thienyl [38, 45, 46, 50, 51]. Below, a synthetic, spectroscopic and structural discussion is presented on derivatives **1**–**4** using comparisons to the literature wherever possible [Recently, the synthesis of **3** has been reported by another research group.] [38b].

2. Experimental

2.1. *General considerations*

All chemicals used herein were used as received from commercial suppliers (Aldrich, Acros, and Junsei companies). The synthetic details for the preparation of the dipyrromethanes and for the BODIPY systems follow literature methods. ^{1}H and ^{13}C NMR spectra were acquired using a Bruker Avance 300 or 400 MHz spectrometer. TMS was used as an internal standard. ^{1}H and ^{13}C NMR spectral signals were calibrated internally by the respective protio impurity or carbon resonance of the CD_2Cl_2 solvent (^{1}H: δ 5.32, ^{13}C: δ 53.8).

2.2. *Syntheses*

Compounds **1**–**4** (figure 1) were prepared by standard protocols [52–54] which involve the use of 2,4-dimethylpyrrole and the respective carboxaldehyde (2- and 3-furaldehyde, 2- and 3-thiophene carboxaldehyde) combined in dichloromethane [53, 54]. [Compound **3** was reported very recently [38b]]. TFA (trifluoroacetic acid) was added at room temperature over the course of 2 h. Dipyrromethanes were used directly for BODIPY synthesis without purification. DDQ was dissolved using toluene and dichloromethane and was added dropwise into the reaction mixture [52]. After stirring for ~4 h, $BF_3 \cdot OEt_2$ was added; triethylamine was subsequently added to give a basic condition (pH = ~8). The reaction mixture was left to stir for ~12 h at room temperature after which the volatiles were removed by rotary evaporation. The solid product was isolated from the residue by way of silica gel column chromatography using dichloromethane/hexane (1 : 1) as eluent and standard work-up (including more rotary evaporation) [38]. The dyes are proven to be pure by standard analytical techniques (Supplementary material). The product yields and NMR characterization are provided below. Low ClogP values (−2.3 to −3.3) were obtained by Molinspiration, suggesting the need for further future modification when applied to neurological living tissue probing (−2.3 (**3**), −2.7 (**4**), −3.0 (**1**), and −3.3 (**2**) [55]. Other calculated pharmacological cheminformatics values were also obtained (Supplementary material).

2.2.1. *4,4-Difluoro-1,3,5,7-tetramethyl-8-(2-furyl)-4-bora-3a,4a-diaza-s-indacene (1)*

33 mg (6.7%) ^{1}H NMR (400 MHz, CD_2Cl_2: δ 5.32): δ 7.65 (dd, $^3J_{H-H} = 1.6$ Hz, $^4J_{H-H} = 0.8$ Hz, $1H_{11}$), 7.56 (dd, $^3J_{H-H} = 3.2$ Hz, $^3J_{H-H} = 1.9$ Hz, $1H_{10}$), 6.49 (dd, $^3J_{H-H} = 3.2$ Hz, $^4J_{H-H} = 0.8$ Hz, $1H_9$), 6.05 (s, $2CH$, H_2), 2.50 (s, $2CH_3$, H_6), 1.60

(s, 2CH_3, H_7) ^{13}C NMR (100 MHz, CD_2Cl_2: δ 53.80): δ 157.21 (s, C_1), 145.36 (dt, $^2J_{C-H} = 9.8$ Hz, $^3J_{C-H} = 7.3$ Hz, C_8), 143.74 (s, C_3), 143.29 (ddd, $^1J_{C-H} = 202.7$ Hz, $^2J_{C-H} = 10.5$ Hz, $^3J_{C-H} = 7.4$ Hz, C_{11}), 133.24 (s, C_4), 128.68 (s, C_5), 121.61 (dm, $^1J_{C-H} = 176.3$ Hz, C_2), 112.16 (ddd, $^1J_{C-H} = 175.8$ Hz, $^2J_{C-H} = 5.8$ Hz, $^3J_{C-H} = 4.1$ Hz, C_9), 111.73 (ddd, $^1J_{C-H} = 175.7$ Hz, $^2J_{C-H} = 13.2$ Hz, $^2J_{C-H} = 3.9$ Hz, C_{10}), 14.82 (q, $^1J_{C-H} = 128.4$ Hz, C_6), 13.13 (dq, $^1J_{C-H} = 127.6$ Hz, $^3J_{C-H} = 2.6$ Hz, C_7) ^{11}B NMR (128.4 MHz, CD_2Cl_2, $BF_3 \cdot OEt_2$: δ 0.00): δ 0.69 (t, $^1J_{B-F} = 32.8$ Hz) ^{19}F NMR (CD_2Cl_2): δ −146.03 (q, $^1J_{B-F} = 32.7$ Hz). MALDI – TOF: $(M - F)^+$ 297.329 (m/z) (Calcd: 295.142).

2.2.2. 4,4-Difluoro-1,3,5,7-tetramethyl-8-(3-furyl)-4-bora-3a,4a-diaza-*s*-indacene (2). 26 mg (5.3%) ^{1}H NMR (400 MHz, CD_2Cl_2: δ 5.32): δ 7.65 (dd, $^3J_{H-H} = 1.7$ Hz, $^4J_{H-H} = 1.7$ Hz, $1H_{10}$), 7.43 (t, $^4J_{H-H} = 1.2$ Hz, $^4J_{H-H} = 1.2$ Hz, $1H_{11}$), 6.41 (dd, $^3J_{H-H} = 1.7$ Hz, $^4J_{H-H} = 0.8$ Hz, $1H_9$), 6.04 (s, 2CH, H_2), 2.50 (s, 2CH_3, H_6), 1.74 (s, 2CH_3, H_7) ^{13}C NMR (100 MHz, CD_2Cl_2: δ 53.80): δ 155.85 (s, C_1), 144.58 (ddd, $^1J_{C-H} = 201.2$ Hz, $^2J_{C-H} = 10.9$ Hz, $^3J_{C-H} = 7.0$ Hz, C_{10}), 143.71 (s, C_3), 140.58 (dt, $^1J_{C-H} = 203.8$ Hz, $^3J_{C-H} = 6.2$ Hz, C_{11}), 133.46 (s, C_5), 132.30 (s, C_4), 121.58 (dm, $^1J_{C-H} = 170.4$ Hz, C_2), 119.03 (ddd, $^2J_{C-H} = 12.4$ Hz, $^2J_{C-H} = 6.3$ Hz, $^3J_{C-H} = 3.1$ Hz, C_8), 111.73 (ddd, $^1J_{C-H} = 176.9$ Hz, $^2J_{C-H} = 13.7$ Hz, $^2J_{C-H} = 5.2$ Hz, C_9), 14.74 (dq, $^1J_{C-H} = 127.4$ Hz, $^3J_{C-H} = 2.7$ Hz, C_6), 14.67 (q, $^1J_{C-H} = 128.1$ Hz, C_7) ^{11}B NMR (128.4 MHz, CD_2Cl_2, $BF_3 \cdot OEt_2$: δ 0.00): δ 0.69 (t, $^1J_{B-F} = 32.9$ Hz) ^{19}F NMR (CD_2Cl_2): δ −146.18 (q, $^1J_{B-F} = 33.0$ Hz) MALDI – TOF: $(M - F)^+$ 297.275 (m/z) (Calcd: 295.142).

2.2.3. 4,4-Difluoro-1,3,5,7-tetramethyl-8-(2-thienyl)-4-bora-3a,4a-diaza-*s*-indacene (3). 39 mg (7.5%) ^{1}H NMR (400 MHz, CD_2Cl_2: δ 5.32): δ 7.54 (dd, $^3J_{H-H} = 5.08$ Hz, $^4J_{H-H} = 1.20$ Hz, $1H_{11}$), 7.15 (dd, $^3J_{H-H} = 5.08$ Hz, $^3J_{H-H} = 3.50$ Hz, $1H_{10}$), 7.01 (dd, $^3J_{H-H} = 3.50$ Hz, $^4J_{H-H} = 1.20$ Hz, $1H_9$), 6.05 (s, 2CH, H_2), 2.53 (s, 2CH_3, H_6), 1.61 (s, 2CH_3, H_7). ^{13}C NMR (100 MHz, CD_2Cl_2: δ 53.80): δ 156.34 (s, C_1), 144.04 (s, C_3), 134.72 (m, C_5), 134.62 (m, C_8), 132.74 (C_4), 128.45 (ddd, $^1J_{C-H} = 167.9$ Hz, $^2J_{C-H} = 9.4$ Hz, $^3J_{C-H} = 5.6$ Hz, C_9), 128.04 (m, C_{10}), 127.90 (m, C_{11}), 121.79 (d, $^1J_{C-H} = 170.8$ Hz, C_2), 14.73 (q, $^1J_{C-H} = 128.3$ Hz, C_6), 13.68 (dq, $^1J_{C-H} = 127.5$ Hz, $^3J_{C-H} = 2.9$ Hz, C_7) ^{11}B NMR (128.4 MHz, CD_2Cl_2, $BF_3 \cdot OEt_2$: δ 0.00): δ 0.71 (t, $^1J_{B-F} = 32.9$ Hz) ^{19}F NMR (CD_2Cl_2): δ −145.94 (q, $^1J_{B-F} = 32.9$ Hz) MALDI – TOF: $(M)^+$ 331.866 (m/z) (Calcd: 330.117), $(M - F)^+$ 313.042 (m/z) (Calcd: 311.119).

2.2.4. 4,4-Difluoro-1,3,5,7-tetramethyl-8-(3-thienyl)-4-bora-3a,4a-diaza-*s*-indacene (4). 43 mg (8.3%) ^{1}H NMR (400 MHz, CD_2Cl_2: δ 5.32): δ 7.53 (dd, $^3J_{H-H} = 5.0$ Hz, $^4J_{H-H} = 3.1$ Hz, $1H_{10}$), 7.25 (dd, $^4J_{H-H} = 2.8$ Hz, $^4J_{H-H} = 1.2$ Hz, $1H_{11}$), 7.00 (dd, $^3J_{H-H} = 4.9$ Hz, $^4J_{H-H} = 1.2$ Hz, $1H_9$), 6.02 (s, 2CH, H_2), 2.50 (s, 2CH_3, H_6), 1.52 (s, 2CH_3, H_7) ^{13}C NMR (100 MHz, CD_2Cl_2: δ 53.80): δ 155.78 (s, C_1), 143.74 (s, C_3), 137.68 (s, C_5), 134.72 (dq, $^3J_{C-H} = 15.2$ Hz, $^3J_{C-H} = 3.6$ Hz, C_8), 132.09 (s, C_4), 127.91 (ddd, $^1J_{C-H} = 168.9$ Hz, $^3J_{C-H} = 8.6$ Hz, $^3J_{C-H} = 4.7$ Hz, C_9), 127.83 (ddd, $^1J_{C-H} = 185.9$ Hz, $^3J_{C-H} = 7.3$ Hz, $^3J_{C-H} = 5.7$ Hz, C_{10}), 124.42 (ddd, $^1J_{C-H} = 185.8$ Hz, $^3J_{C-H} = 8.8$ Hz, $^3J_{C-H} = 5.1$ Hz, C_{11}), 121.44 (d, $^1J_{C-H} = 167$ Hz, C_2), 14.67 (q, $^1J_{C-H} = 128$ Hz, C_6), 13.81 (dq, $^1J_{C-H} = 127.3$ Hz, $^3J_{C-H} = 2.7$ Hz, C_7) ^{11}B NMR

(128.4 MHz, CD_2Cl_2, $BF_3 \cdot OEt_2$: δ 0.00): δ 0.72 (t, $^1J_{B-F} = 33.0$ Hz) ^{19}F NMR (CD_2Cl_2): −146.23 (q, $^1J_{B-F} = 33.0$ Hz) MALDI – TOF: $(M)^+$ 331.864 (m/z) (Calcd: 330.117), $(M - F)^+$ 313.042 (m/z) (Calcd: 313.046).

3. Results and discussion

3.1. *NMR characterization*

Various NMR spectroscopic data of **1–4** were obtained in CD_2Cl_2: ^1H, ^{13}C, ^{13}C–^1H coupled NMR, and 2-D NMR spectra including ^1H–^1H COSY, ^1H–^1H NOESY, ^1H–^{13}C HSQC, and ^1H–^{13}C HMBC. Further, ^{19}F and ^{11}B NMR spectra were also acquired (Supplementary material). Reproductions of certain representative spectra are presented and discussed below; more appear in the Supplementary material. ^1H, ^{13}C, ^{11}B, and ^{19}F nuclei were assigned spectrally. First, all samples reveal an ^{11}B NMR spectroscopic resonance located at 0.69 ppm (**1**, **2**) and 0.71 ppm (**3**, **4**). Coupling constants were ~33 Hz for all compounds (**1–4**) (Supplementary material). Triplets 1 : 2 : 1 are present from boron coupling with the adjacent fluorines ($^1J_{B-F}$) signifying the presence of a difluoroboryl unit consistent with the characteristic bright redness known for this compound class. In the ^{19}F NMR spectra, the peaks reveal a standard 1 : 1 : 1 : 1 quartet in the region of −145 ppm to −146 ppm for **1–4**. The nature of coupling comes from the proximity of the boron ($^{11}B = 80.1\%$ abundance), possessing a nuclear spin of 3/2. Coupling constants, this time as $^1J_{B-F}$, were reconfirmed to be ~33 Hz for **1–4**. With respect to the ^1H NMR spectroscopic resonances, the BODIPY system cores (figure 1) have only two methine and four methyl proton signals. The chemical shift of this hydrogen (H_2) is about 6.0 ppm for **1–4**. This group is distal to the aryl substituent; there are minor but detectable *meso*-functional group differences. The BODIPY core has four methyl groups, broken down into two chemical shift equivalent sets (positions 6 and 7) (figure 1). The proton shifts differed most for the 7-position protons found more upfield (table 1). Compound **2** contains the proton H_7 as the most deshielded of the four compounds, possibly owing to the fact that the BODIPY-aryl dihedral angle is smaller (*vide infra*), and a more effective donation from the *meso*-ring to the methyl H_7 protons may be possible. The *meso*-substituted rings each have three hydrogen atoms. These protons are easily assigned by ^1H–^1H COSY NMR spectroscopy. In the furyl case, the peak gap is bigger than in the thienyl cases (figure 2). The furyl oxygen is electron withdrawing and polarizing, reflected in the NMR: the nearest H-atom is somewhat deshielded; other H atoms are *relatively shielded* possibly due to the reducing ring current. In the ^1H–^1H NOESY NMR spectra, β-methyl-substituted protons share a

Table 1. Chemical shifts (ppm) of BODIPY core protons 7, 2, and 6 (decreasing differences) for **1–4** (CD_2Cl_2).

Proton/Compound No.	**7**	**2**	**6**
1 (2F)	1.60	<u>6.05</u>	2.50
2 (3F)	<u>1.74</u>	6.04	2.50
3 (2T)	1.61	<u>6.05</u>	<u>2.53</u>
4 (3T)	1.52	6.02	2.50

The underlined values are the largest ones found for each value in the set of compounds.

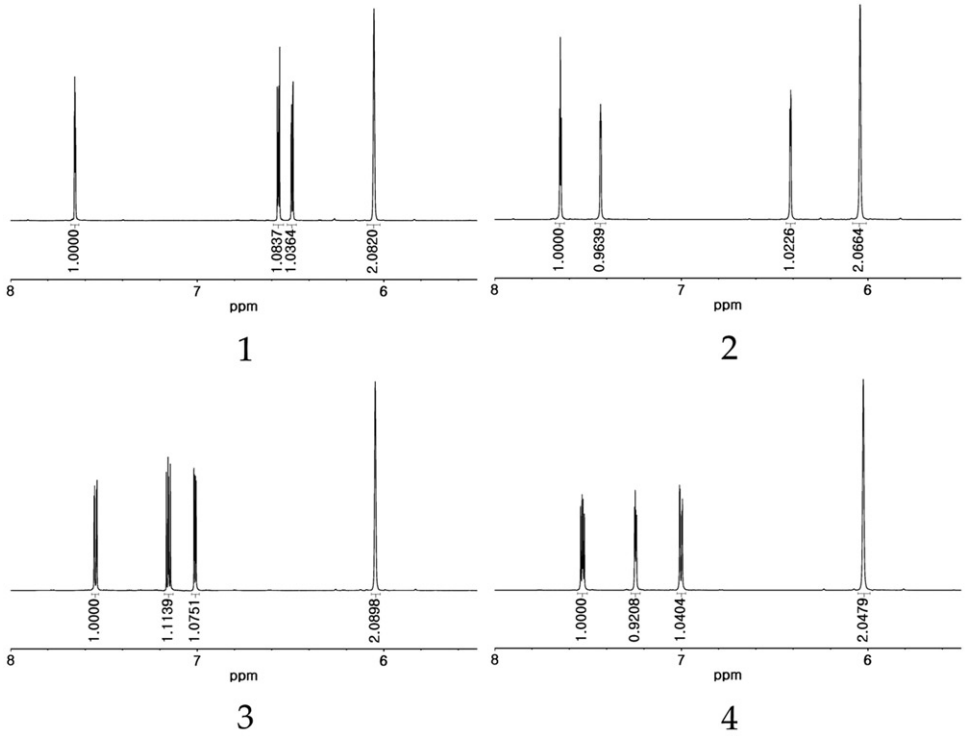

Figure 2. ^{1}H NMR spectra of the aromatic region ($\delta = 5.5$–8.0) for **1–4** in CD_2Cl_2.

crosspeak with *meso*-heterocyclic protons (figure 3). The BODIPY core proton (H_2) is interacting with α- and β-methyl protons for **1–4**. H_7 is coupled with the *meso*-ring where the average through-space distance is short. *Meso*-ring protons are also correlated with H_7 by NOESY.

^{13}C and ^{1}H-coupled ^{13}C NMR spectra were also obtained for **1–4**. Some multiple through-bond coupling is confirmed. In **4**, C_6 and C_7 are $^{3}J_{C-H}$ coupled to H_2. Also, H_6 and H_7 couple with C_6 and C_7, respectively. The C_6 and C_7 peaks in the ^{13}C NMR spectrum are doublets-of-quartets as predicted; but, the C_6 signal is broadened. Carbon C_2 has one hydrogen atom (H_2); also, H_6 and H_7 are proximal to C_2. H_6 and H_7 are coupling minimally, so the C_2 signal is shown more as a broad doublet. In the ^{13}C NMR spectrum, C_9, C_{10}, and C_{11} peaks are complex signals which relate the thiophene protons to each other. Further, all carbon peaks were assigned through ^{1}H–^{13}C HSQC NMR and ^{1}H–^{13}C HMBC NMR spectroscopies. In the HSQC spectrum, crosspeaks were located for directly connected C–H groups ($^{1}J_{C-H}$) (figure 4). For **3** and **4** there is a more linear HSQC profile of crosspeaks, whereas for **1** and **2**, the carbon–proton signal correlation is found to be more separated. Quaternary carbon peaks are assignable from the HMBC spectra (figure 5). In **4**, C_1 is more closely and strongly coupled with H_6 than with H_7. C_3 is closer and more strongly coupled to H_7 than it is to H_6. The nucleus of C_5 couples with H_{11} and H_9. C_8 couples with H_9, H_{10}, and H_{11}. Further, C_4 couples with H_2 and H_7. Related coupling described above for **4** can also be found for **1–3**.

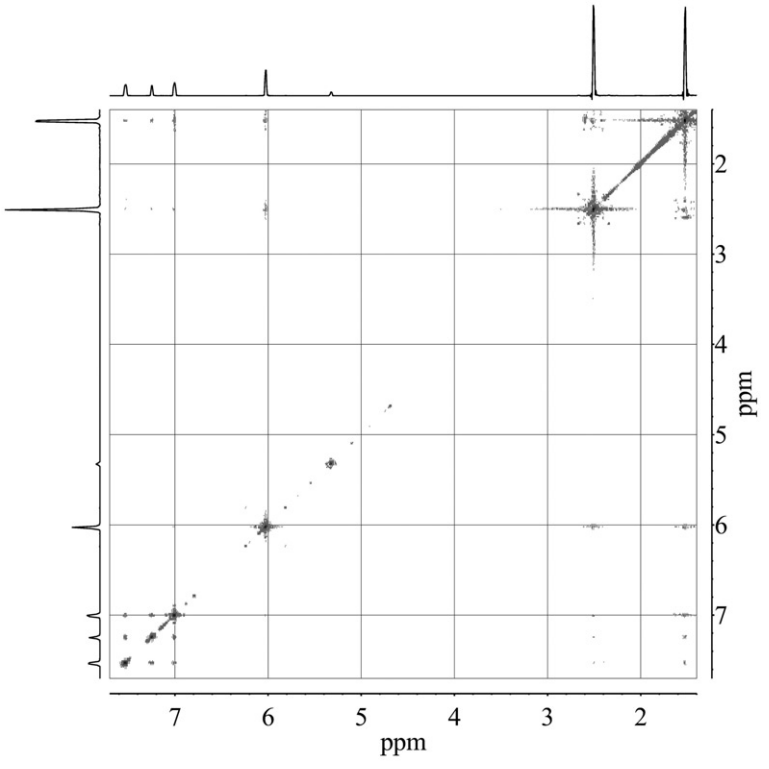

Figure 3. ^{1}H–^{1}H NOESY NMR spectrum for **4** in CD_2Cl_2.

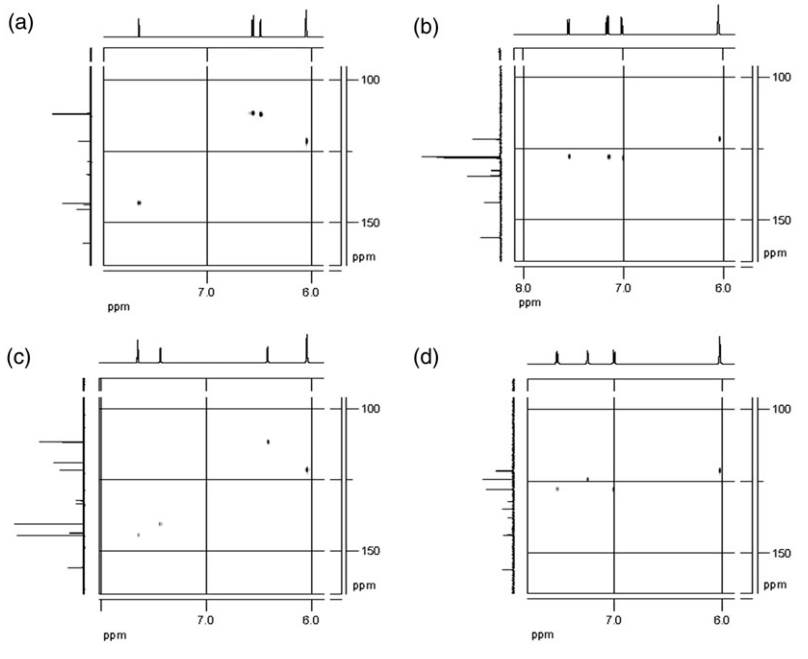

Figure 4. Section of the ^{1}H–^{13}C HSQC NMR spectra for **1–4** in CD_2Cl_2. Compounds **1** (a), **3** (b), **2** (c), and **4** (d), in order of electron-withdrawing differences.

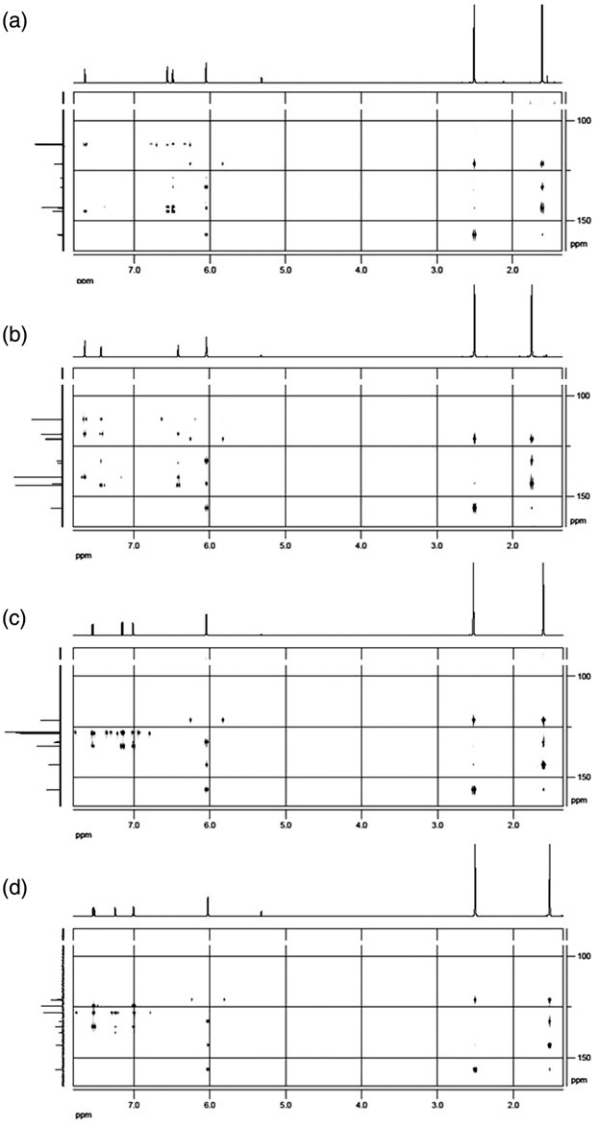

Figure 5. Portions of ^{1}H–^{13}C HMBC NMR spectra for **1–4**. Compounds **1** (a), **3** (b), **2** (c), and **4** (d).

Species **1–4** are roughly an order of magnitude more fluorescent than their previously reported *non-methylated* counterparts [46]. Characteristic absorption ($\lambda_{ABS} = 500$–514 nm) and emission maxima ($\lambda_{EM,MAX} = 513$–528 nm) were determined (figure 6, table 2). The spectrum for **3** is less red-diffused revealing that the rotor is sterically held upright. The optics of the 2-furyl/2-thienyl-containing compounds show absorptions slightly toward longer wavelength than their 3-furyl/3-thienyl counterparts. For both the 2- and 3-substituted compounds, partial extended π-conjugation is feasible through a *meso*meric effect, provided that the flanking methyl groups (1 and 7 positions) of the dipyrrin do not hinder ring rotation too severely. In recent work on *fully* alkylated

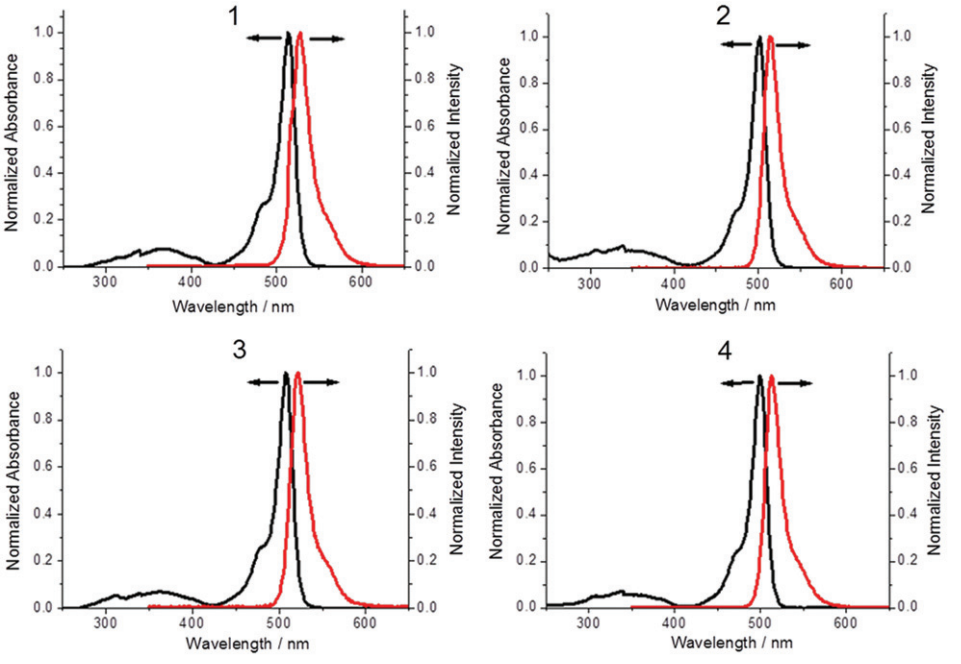

Figure 6. Normalized absorption spectra (black graph) and normalized fluorescence spectra (red graph) for **1–4** in acetonitrile (conc. $= 5.0 \times 10^{-6}$ mol L^{-1}). The red emission spectrum will appear grey in the printed black and white version.

Table 2. Photophysical data for **1–4** collected in MeCN.

Compound	λ_{ABS} (nm)	λ_{EM} (nm)
1 (2F)	514	528
2 (3F)	501	514
3 (2T)	508	528
4 (3T)	500	513

BODIPY derivatives containing oligothiophene moieties at the *meso*-position, unhindered thiophene rotation is used to explain the electronic coupling between the two subunits [42]. There is no reason that the same notion does not apply here for derivatives **1–4** to enhance conjugation. However, since small bathochromic shifts are observed for both the 2-furyl/2-thienyl derivatives, a secondary electronic effect must act on the dipyrrin core.

3.2. *Crystallographic studies*

Single-crystal X-ray crystal structures of **1–4** were obtained. Crystals were prepared *via* slow evaporation out of dichloromethane/methanol at room temperature. 2-Thienyl- and 2-furyl-substituted compounds were generated as thin plates, whereas the crystals

of the 3-thienyl and 3-furyl-based compounds grew as needles. Compound **1** is found in the orthorhombic *Pbca* space group with cell dimensions $a = 12.9053(9)$ Å, $b = 12.4096(8)$ Å, and $c = 19.5554(14)$ Å. Compound **2** is monoclinic and is found in the common $P2_1/n$ space group with cell dimensions $a = 12.053(2)$ Å, $b = 6.8102(12)$ Å, $c = 19.063(3)$ Å, and $\beta = 101.338(9)^\circ$. Compound **3** is monoclinic and is found in the *Pc* space group with cell dimensions $a = 6.7332(4)$ Å, $b = 18.6120(10)$ Å, $c = 13.1048(7)$ Å, and $\beta = 93.026(3)^\circ$ (this molecule could also be solved in P_1 (4 independent molecules), but not $P\bar{1}$ or $P2/c$). Compound **4** is monoclinic and is found in the common $P2_1/n$ space group with cell dimensions $a = 10.906(2)$ Å, $b = 12.813(3)$ Å, $c = 13.036(3)$ Å, and $\beta = 112.295(12)^\circ$. Compounds **1** and **4** revealed aspects of crystallographic disorder related to the unsymmetric nature of the heterocyclic rotor (figure 7). This rotor was modeled in two parts as performed by us in previous related work. After close scrutiny, **2** and **3** were determined not to involve disorder. Formal single-atomic changes alter slightly the crystal packing. Also, there is a 2-/3-aryl difference when considering crystallographic packing. The larger atom naturally gives a larger unit cell volume (V)-to-unit number (Z) ratio and calculated density values (table 3). When changing formally from **2** to **4**, the unit cell volume (V)-to-unit number (Z) ratio increases, but the calculated density decreases.

There are many different intramolecular dihedral angles present in the solid state (table 3). The most important angle is that for the BODIPY-aryl rotor (mpln 6–7). Comparing with a previous report [46], angular values here between the *meso*-substituted heterocycle ring and the BODIPY core are more perpendicular. Most of these compounds have a dihedral angle of ~90°; this is reasonable based on values found for the bulky mesityl (~75°) or *o*-tolyl group (~85°) geometries [34]. Herein, we tried to break apart the packing effects of atom *versus* effect of the rotor torsion angle for **1**–**4**. Compound **2** has the smallest dihedral angle between *mean planes* 6 and 7 and the largest value of density and the V/Z ratio for the four compounds. The dihedral angle and *meso*-substituted ring size are related to crystallographic packing. In the thienyl compounds, the 3-thienyl substituted compound (**4**) has a ring crosslength (4.04 Å) larger than that for the 2-thienyl compound (**3**) (3.54 Å). However, the dihedral angle between the *meso*-substituted heterocyclic ring and the BODIPY core are similar (**3**: 87.3°, **4**: 80.4°). Ring size is more effective than the dihedral angle in affecting the value of density and the V/Z ratio in this case. For the furyl compounds, the 3-furyl substituted compound (**2**) has a ring crosslength (3.98 Å) larger than that for the 2-furyl **1** (3.07 Å). Further, the dihedral angle between the *meso*-substituted heterocyclic ring and the BODIPY core are 88.6° (**1**) and 81.1° (**2**). In this case, both the ring size and dihedral angle are affected, but the more important factor appears to be the dihedral angle. After all, when comparing between **2** and **4**, the ring size is similar but the dihedral angle is different. These lead to different values of density and the V/Z ratio (table 3). While the ring crosslength becomes larger, density is reduced. But, in **1** and **2**, density was increased even though the ring crosslength increased. In this case, the dihedral angle factor is more important than the ring size factor. But for **3** and **4**, the density and dihedral angle decreased; the ring size increase was relatively small compared with that found between **1** and **2** thought to be related to the larger atom size for sulfur. For these reasons, the atom size effect can override the secondary rotor angle effect.

Here, we can discuss certain other dihedral angles between the congeners and isomers. Puckering can be accounted for by the dihedral angles 1–2 (°) or 5–6 (°). For 1–2 (°) the

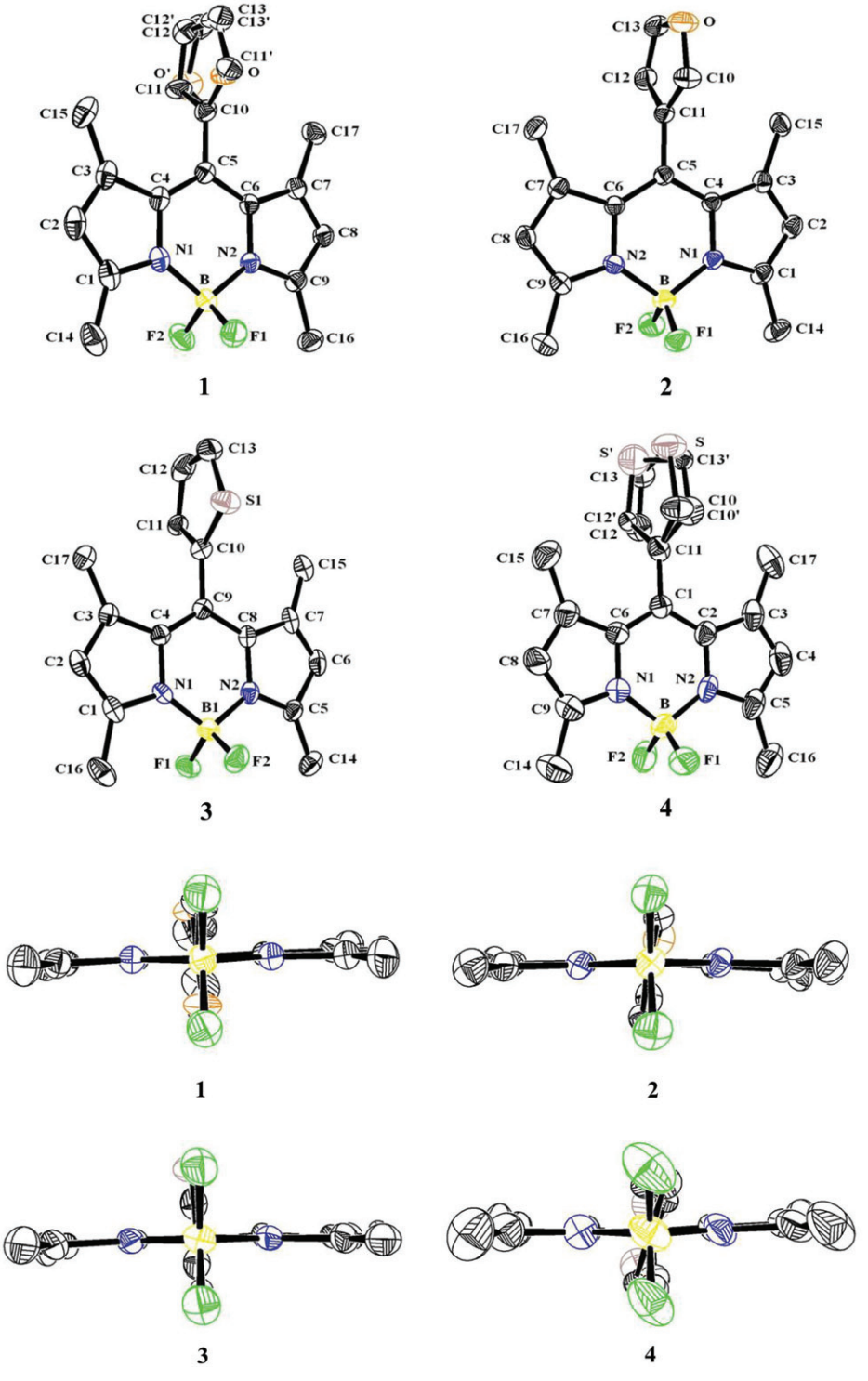

Figure 7. Top (top) and front (bottom) views of the crystallographic molecular structures of **1–4**. Compound **1**: orthorhombic, *Pbca*, $a = 12.9053(9)$ Å, $b = 12.4096(8)$ Å, $c = 19.5554(14)$ Å. Compound **2**: monoclinic, $P2_1/n$, $a = 12.053(2)$ Å, $b = 6.8102(12)$ Å, $c = 19.063(3)$ Å, $\beta = 101.338(9)^\circ$. Compound **3**: monoclinic, *Pc*, $a = 6.7332(4)$ Å, $b = 18.6120(10)$ Å, $c = 13.1048(7)$ Å, $\beta = 93.026(3)^\circ$. Compound **4**, monoclinic, $P2_1/n$, $a = 10.906(2)$ Å, $b = 12.813(3)$ Å, $c = 13.036(3)$ Å, $\beta = 112.295(12)^\circ$. Evidence of crystallographic disorder is shown for **1** and **4**.

Table 3. Selected parameters for crystallographic data for **1–4**.

	Crystal system	Space group	V (Å^3)	Z	V/Z (Å^3/molecule)	P_{calcd} (Mgm^{-3})
1	Orthorhombic	*Pbca*	3131.8(4)	8	391.5	1.332
2	Monoclinic	$P2_1/n$	1534.2(5)	4	383.6	1.360
3	Monoclinic	*Pc*	1639.98(16)	4	410.0	1.337
4	Monoclinic	$P2_1/n$	1685.4(6)	4	421.4	1.301

Table 4. Certain dihedral angles between *mean planes* for **1–4**.

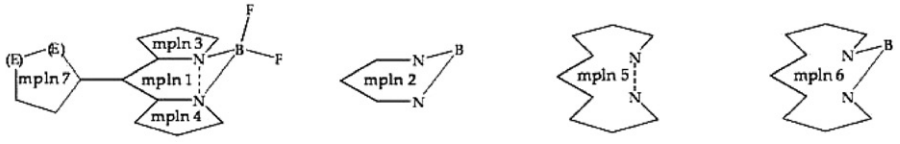

Mean planes	1–2 (°)	3–4 (°)	5–6 (°)	6–7 (°)
1	0.2	2.7	0.0	88.6
2	0.2	5.1	0.3	81.1
3	0.4	4.0	0.4	87.3
4	0.5	4.0	0.4	80.4

biggest deviation is for **3** and **4**, but it is of only 0.4°. Interestingly, the 5–6 (°) difference for these same two compounds is also the same. It appears from table 4 that the puckering angle and "wing" tip tilting are independent. The greatest angle between 3 and 4 (°) is found for **2** (5.1°). Crystallographic packing was also assessed (figures 8–11). There appears to be no significant specific intermolecular interactions found; no solvent molecules are present. The inter-layering arrays of **1–4** are shown below in which distances are provided for reference.

4. Conclusion

We have prepared several closely related BODIPY derivatives to further quantify the heteroatom effect structurally, optically (UV-Vis and emission), and by NMR spectroscopy. In these compounds, the 8-aryl position bears a heterocycle containing oxygen or sulfur at one of two different positions. Specifically, the compounds were characterized in solution (CD_2Cl_2) through thorough NMR spectroscopy (^{1}H, ^{13}C, ^{11}B, ^{19}F, ^{13}C–H coupled, ^{1}H–^{1}H COSY, ^{1}H–^{13}C HSQC, and ^{1}H–^{13}C HMBC). Optically, the UV-Vis and emission spectral profiles were confirmed. Species **1–4** are approximately one order of magnitude more fluorescent than the non-methylated ones previously reported [37, 46]. Solid-state data by four separate X-ray diffraction studies were obtained. The molecules in the asymmetric unit for **2** pack more effectively in the crystal affording the largest calculated density for the series. Various angles were discussed:

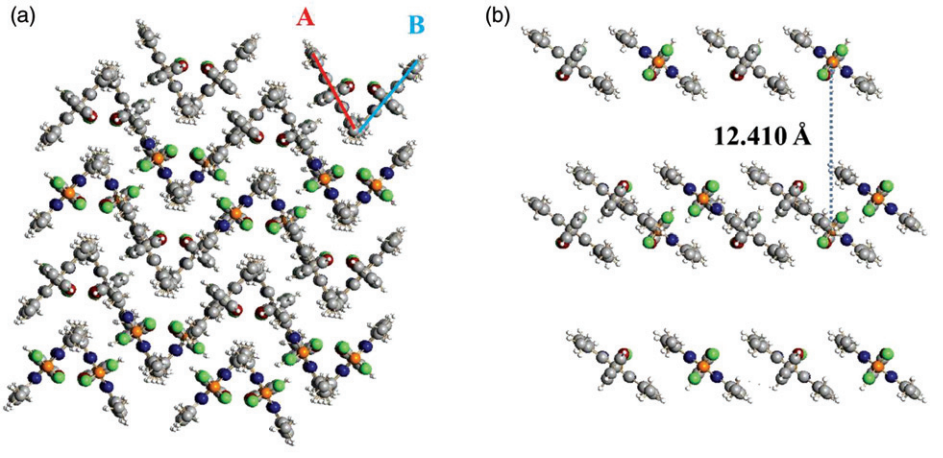

Figure 8. Packing diagram of **1:** (a) overall packing diagram and (b) one molecular component to overall packing.

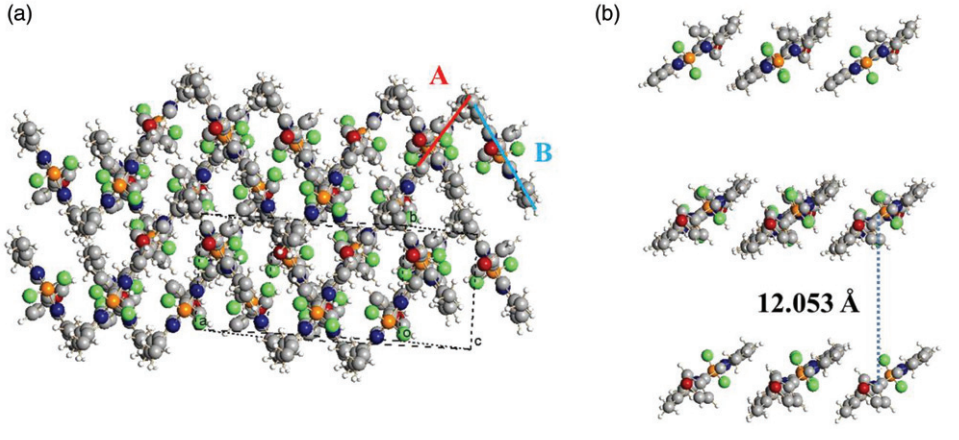

Figure 9. Packing diagram of **2:** (a) overall packing diagram and (b) one molecular component to overall packing.

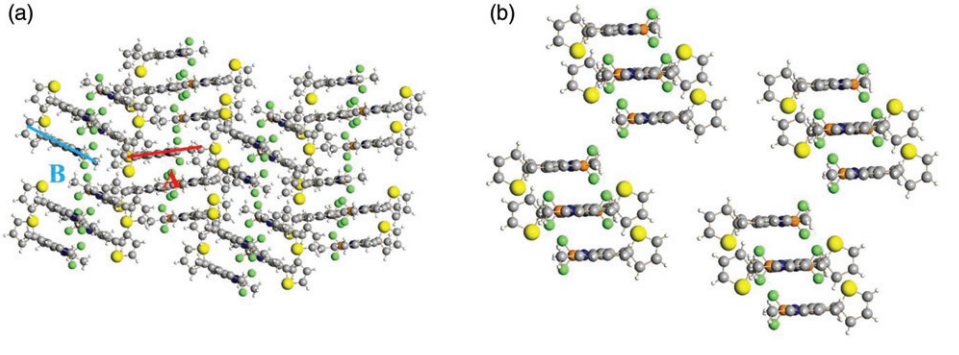

Figure 10. Packing diagram of **3:** (a) overall packing diagram and (b) one molecular component to overall packing.

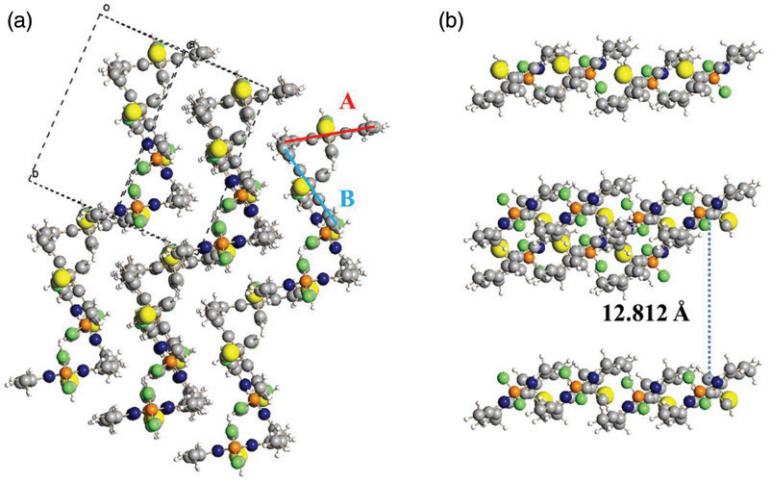

Figure 11. Packing diagram of **4:** (a) overall packing diagram and (b) one molecular component to overall packing.

importantly, formally when the O or S is placed closer (from 3- to 2-substitution), the 6–7 angle becomes more orthogonal: compound $\mathbf{2} \rightarrow \mathbf{1}$: $81.1^\circ \rightarrow 88.6^\circ$; compound $\mathbf{4} \rightarrow \mathbf{3}$: $80.4^\circ \rightarrow 87.3^\circ$. NMR spectroscopic data acquired revealed subtle differences in ^{1}H NMR spectra in the dipyrrin region for **1**–**4** because of the affect of the electron-withdrawing groups at the *meso*-position. The tuning of the excited state properties of BODIPY compounds is a play-off between electronic and structure-based effects which we hope to exploit in molecular neurodegenerative disease research studies *via* future BF_2-chelate derivatization.

Supplementary material

Reproductions of NMR spectra, further crystallographic information, etc are available in supplementary file. The Crystallographic data obtained herein has been deposited with the Cambridge Crystallographic Data Centre, CCDC. Structures CCDC 795900–2, 791925 have been assigned. These data can be obtained free of charge from The Cambridge Crystallographic Data Centre (12 Union Road, Cambridge, CB2 1EZ, UK, +441223336408) *via* www.ccdc.cam.ac.uk/data_request/cif

Acknowledgments

Professor David G. Churchill, Director of the Molecular Logic Gate Laboratory, acknowledges funding from the National Research Foundation (Grant # 2009−0070330, 2010−0013660, 2011–0017280). Dr Andrew C. Benniston acknowledges the support of the University of Newcastle. The authors thank Professor

Youngkyu Do for enabling the X-ray determination for **1**–**4**. Additional funding has been granted from Hak-Jae Kim, CEO of Dong-a Pencil Co., Daejeon, Korea.

References

[1] A. Treibs, F.H. Kreuzer. *Liebigs Ann. Chem.*, **718**, 208 (1968).
[2] A. Loudet, K. Burgess. *Chem. Rev.*, **107**, 4891 (2007).
[3] G. Ulrich, R. Ziessel, A. Harriman. *Angew. Chem., Int. Ed.*, **47**, 1184 (2008).
[4] F. Bergstrom, P. Hagglof, J. Karolin, T. Ny, L.B.A. Johansson. *Proc. Natl Acad. Sci. USA*, **96**, 12477 (1999).
[5] J. Karolin, L.B.A. Johansson, L. Strandberg, T. Ny. *J. Am. Chem. Soc.*, **116**, 7801 (1994).
[6] H. Kobayashi, M. Ogawa, R. Alford, P.L. Choyke, Y. Urano. *Chem. Rev.*, **110**, 2620 (2010).
[7] Z.G. Li, R. Bittman. *J. Org. Chem.*, **72**, 8376 (2007).
[8] Z.G. Li, E. Mintzer, R. Bittman. *J. Org. Chem.*, **71**, 1718 (2006).
[9] Q.L. Meng, D.H. Kim, X.P. Bai, L.R. Bi, N.J. Turro, J.Y. Ju. *J. Org. Chem.*, **71**, 3248 (2006).
[10] E.J. Merino, K.M. Weeks. *J. Am. Chem. Soc.*, **127**, 12766 (2005).
[11] C. Peters, A. Billich, M. Ghobrial, K. Hogenauer, T. Ullrich, P. Nussbaumer. *J. Org. Chem.*, **72**, 1842 (2007).
[12] R. Ziessel, G. Ulrich, A. Harriman. *New J. Chem.*, **31**, 496 (2007).
[13] A. Coskun, E. Deniz, E.U. Akkaya. *Org. Lett.*, **7**, 5187 (2005).
[14] T.A. Golovkova, D.V. Kozlov, D.C. Neckers. *J. Org. Chem.*, **70**, 5545 (2005).
[15] S. Atilgan, T. Ozdemir, E.U. Akkaya. *Org. Lett.*, **10**, 4065 (2008).
[16] M. Baruah, W.W. Qin, N. Basaric, W.M. De Borggraeve, N. Boens. *J. Org. Chem.*, **70**, 4152 (2005).
[17] A. Coskun, E.U. Akkaya. *J. Am. Chem. Soc.*, **127**, 10464 (2005).
[18] T.W. Hudnall, F.P. Gabbai. *Chem. Commun.*, 4596 (2008).
[19] K. Krumova, P. Oleynik, P. Karam, G. Cosa. *J. Org. Chem.*, **74**, 3641 (2009).
[20] J.B. Wang, X.H. Qian. *Org. Lett.*, **8**, 3721 (2006).
[21] Y.K. Wu, X.J. Peng, B.C. Guo, J.L. Fan, Z.C. Zhang, J.Y. Wang, A.J. Cui, Y.L. Gao. *Org. Biomol. Chem.*, **3**, 1387 (2005).
[22] K. Yamada, Y. Nomura, D. Citterio, N. Iwasawa, K. Suzuki. *J. Am. Chem. Soc.*, **127**, 6956 (2005).
[23] M.J. Yuan, W.D. Zhou, X.F. Liu, M. Zhu, J.B. Li, X.D. Yin, H.Y. Zheng, Z.C. Zuo, C. Ouyang, H.B. Liu, Y.L. Li, D.B. Zhu. *J. Org. Chem.*, **73**, 5008 (2008).
[24] L. Zeng, E.W. Miller, A. Pralle, E.Y. Isacoff, C.J. Chang. *J. Am. Chem. Soc.*, **128**, 10 (2006).
[25] S. Mula, A.K. Ray, M. Banerjee, T. Chaudhuri, K. Dasgupta, S. Chattopadhyay. *J. Org. Chem.*, **73**, 2146 (2008).
[26] T. Yogo, Y. Urano, Y. Ishitsuka, F. Maniwa, T. Nagano. *J. Am. Chem. Soc.*, **127**, 12162 (2005).
[27] A. Loudet, R. Bandichhor, L.X. Wu, K. Burgess. *Tetrahedron*, **64**, 3642 (2008).
[28] K. Tan, L. Jaquinod, R. Paolesse, S. Nardis, C. Di Natale, A. Di Carlo, L. Prodi, M. Montalti, N. Zaccheroni, K.M. Smith. *Tetrahedron*, **60**, 1099 (2004).
[29] G. Ulrich, C. Goze, M. Guardigli, A. Roda, R. Ziessel. *Angew. Chem., Int. Ed.*, **44**, 3694 (2005).
[30] S. Erten-Ela, M.D. Yilmaz, B. Icli, Y. Dede, S. Icli, E.U. Akkaya. *Org. Lett.*, **10**, 3299 (2008).
[31] F.R. Li, S.I. Yang, Y.Z. Ciringh, J. Seth, C.H. Martin, D.L. Singh, D.H. Kim, R.R. Birge, D.F. Bocian, D. Holten, J.S. Lindsey. *J. Am. Chem. Soc.*, **120**, 10001 (1998).
[32] T. Rousseau, A. Cravino, T. Bura, G. Ulrich, R. Ziessel, J. Roncali. *Chem. Commun.*, 1673 (2009).
[33] M.D. Yilmaz, O.A. Bozdemir, E.U. Akkaya. *Org. Lett.*, **8**, 2871 (2006).
[34] H.L. Kee, C. Kirmaier, L.H. Yu, P. Thamyongkit, W.J. Youngblood, M.E. Calder, L. Ramos, B.C. Noll, D.F. Bocian, W.R. Scheidt, R.R. Birge, J.S. Lindsey, D. Holten. *J. Phys. Chem. B*, **109**, 20433 (2005).
[35] S.H. Lim, C. Thivierge, P. Nowak-Sliwinska, J.Y. Han, H. van den Bergh, G. Wagnieres, K. Burgess, H.B. Lee. *J. Med. Chem.*, **53**, 2865 (2010).
[36] V.R. Donuru, G.K. Vegesna, S. Velayudham, S. Green, H.Y. Liu. *Chem. Mater.*, **21**, 2130 (2009).
[37] S.H. Choi, K. Kim, J. Lee, Y. Do, D.G. Churchill. *J. Chem. Crystallogr.*, **37**, 315 (2007).
[38] (a) E. Peña-Cabrera, A. Aguilar-Aguilar, M. Gonzalez-Dominguez, E. Lager, R. Zamudio-Vazquez, J. Godoy-Vargas, F. Villanueva-Garcia. *Org. Lett.*, **9**, 3985 (2007); (b) Y. Chen, J. Zhao, H. Guo, L. Xie. *J. Org. Chem.*, **77**, 2192 (2012); (c) X. Qu, Q. Liu, X. Ji, H. Chen, Z. Zhou, Z. Shen. *Chem. Commun.*, **48**, 4600 (2012); (d)H. Saji, M. Ono, H. Kimura, H. Kawashima, PCT Int. Appl., WO 2010125907 A1 20101104 (2010); (e) Y. Xiao, D. Zhang, *Faming Zhuanli Shenqing Gongkai Shuomingshu* (2009), CN 101565554 A 20091028.

[39] D. Collado, J. Casado, S.R. Gonzalez, J.T.L. Navarrete, R. Suau, E. Perez-Inestrosa, T.M. Pappenfus, M.M.M. Raposo. *Chem. Eur. J.*, **17**, 498 (2011).
[40] A.C. Benniston, G. Copley, A. Harriman, R. Ryan. *J. Mater. Chem.*, **21**, 2601 (2011).
[41] S. Zrig, P. Remy, B. Andrioletti, E. Rose, I. Asselberghs, K. Clays. *J. Org. Chem.*, **73**, 1563 (2008).
[42] A.C. Benniston, G. Copley, A. Harriman, D.B. Rewinska, R.W. Harrington, W. Clegg. *J. Am. Chem. Soc.*, **130**, 7174 (2008).
[43] J. Banuelos, I.J. Arroyo-Cordoba, I. Valois-Escamilla, A. Alvarez-Hernandez, E. Peña-Cabrera, R.R. Hu, B.Z. Tang, I. Esnal, V. Martinez, I.L. Arbeloa. *RSC Adv.*, **1**, 677 (2011).
[44] E. Lager, J.Z. Liu, A. Aguilar-Aguilar, B.Z. Tang, E. Peña-Cabrera. *J. Org. Chem.*, **74**, 2053 (2009).
[45] S. Kim, T.Y. Ohulchanskyy, A. Baev, P.N. Prasad. *J. Mater. Chem.*, **19**, 3181 (2009).
[46] (a) K. Kim, C. Jo, S. Easwaramoorthi, J. Sung, D.H. Kim, D.G. Churchill. *Inorg. Chem.*, **49**, 4881 (2010); (b) A.P. Singh, K.M. Lee, D.P. Murale, T. Jun, H. Liew, Y.-H. Suh, D.G. Churchill. *Chem. Commun.*, **48**, 7298 (2012); (c) A.P. Singh, K.M. Lee, K. Kim, T. Jun, D.G. Churchill. *Eur. J. Org. Chem.*, **5**, 931 (2012).
[47] D.G. Churchill, S.H. Choi, K. Pang, K. Kim. KR, 0908930 B1 20090715 (2009) (Korean Patent).
[48] S.H. Choi, K. Kim, J. Jeon, B. Meka, D. Bucella, K. Pang, S. Khatua, J. Lee, D.G. Churchill. *Inorg. Chem.*, **47**, 11071 (2008).
[49] S.H. Choi, K. Pang, K. Kim, D.G. Churchill. *Inorg. Chem.*, **46**, 10564 (2007).
[50] A.J. Cui, Y.C. Jia, Q. Chen, M.Y. He. *Huaxue Shiji*, **33**, 799 (2011).
[51] T.K. Khan, M.R. Rao, M. Ravikanth. *Eur. J. Org. Chem.*, **12**, 2314 (2010).
[52] C. Brückner, V. Karunaratne, S.J. Rettig, D. Dolphin. *Can. J. Chem. – Rev. Canadienne Chim.*, **74**, 2182 (1996).
[53] C.H. Lee, J.S. Lindsey. *Tetrahedron*, **50**, 11427 (1994).
[54] R.W. Wagner, J.S. Lindsey. *Pure Appl. Chem.*, **68**, 1373 (1996).
[55] *Molinspiration Cheminformatics*, Bratislava, Slovak Republic. Available online at: http://www.molinspiration.com (accessed September 2012).